

# Puzzling X-rays from the new colliding wind binary WR 65 (WC9d)

L. M. Oskinova<sup>\*</sup> & W.-R. Hamann

Potsdam University, Universitätsstandort Golm, Haus 28, Potsdam, 14476 Germany

Accepted 2008 July 29. Received 2008 July 25; in original form 2008 July 7

## ABSTRACT

We report the discovery of variability in the X-ray emission from the Wolf-Rayet type star WR 65. Using archival *Chandra* data spanning over 5 yr we detect changes of the X-ray flux by a factor of 3 accompanied by changes in the X-ray spectra. We believe that this X-ray emission originates from wind-wind collision in a massive binary system. The observed changes can be explained by the variations in the emission measure of the hot plasma, and by the different absorption column along the binary orbit. The X-ray spectra of WR 65 display prominent emission features at wavelengths corresponding to the lines of strongly ionized Fe, Ca, Ar, S, Si, and Mg. WR 65 is a carbon rich WC9d star that is a persistent dust maker. This is the first investigation of any X-ray spectrum for a star of this spectral type. There are indications that the dust and the complex geometry of the colliding wind region are pivotal in explaining the X-ray properties of WR 65.

**Key words:** stars:early-type – stars:Wolf-Rayet – stars:individual:WR 65 – X-ray:stars

## 1 INTRODUCTION

More than 54% of all Wolf-Rayet (WR) stars are in binary systems that consist of a WR and an OB-type star (Wallace 2007). The collision between two stellar winds in these systems produces characteristic signatures in different wavelength bands that can include non-thermal radio emission (Eichler & Usov 1993), copious and variable X-rays (Stevens, Blondin & Pollock 1992), and dust emission in the infrared (IR) (Williams, van der Hucht & The 1987).

Subject of this *Letter* is the WC9d star WR 65. Williams, van der Hucht & The (1987) reported the presence of warm dust in this object. They discussed that in early-type WC stars an increase in the wind density provided by e.g. shock compression in colliding winds in binary systems may be sufficient to result in grain formation. Zubko (1998) found no need to invoke binarity to explain the presence of dust in late WC stars. He fitted the observed IR spectrum of WR 65 assuming a single star with stellar mass-loss in the form of dust with  $\dot{M}_d = 5.4 \times 10^{-10} M_\odot \text{yr}^{-1}$  and surrounded by a dust shell with an inner radius of  $520 R_*$ . Leitherer, Chapman & Koribalski (1997) detected radio emission from WR 65, but could not constrain its spectral index.

In a previous paper (Oskinova et al. 2003) we demonstrated that single WC type stars are X-ray quiet and proposed that all X-ray active WC stars must be in binary systems. X-ray emission from WR 65 was detected and tentatively explained as a result of wind-wind collision. In this paper we report on the X-ray light curve of WR 65 and changes in its X-ray spectra that unambiguously confirm its status as a colliding-wind binary (CWB).

**Table 1.** Coordinates of WR 65 from different sources

Ref	Band	RA J2000	DEC J2000
Simbad	opt.	15 <sup>h</sup> 13 <sup>m</sup> 41 <sup>s</sup> .68	−59° 11′ 43″.3
Chapman et al. (1999)	radio	15 <sup>h</sup> 13 <sup>m</sup> 41 <sup>s</sup> .49	−59° 11′ 43″.8
<i>Chandra</i> HRC-I	X-ray	15 <sup>h</sup> 13 <sup>m</sup> 41 <sup>s</sup> .76	−59° 11′ 44″.1
Catalog USNO-B1.0	opt.	15 <sup>h</sup> 13 <sup>m</sup> 41 <sup>s</sup> .73	−59° 11′ 43″.4

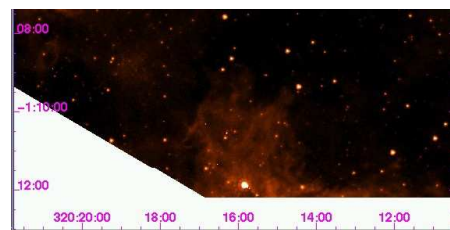


**Figure 1.** Archival *Spitzer* image ( $8 \mu\text{m}$ ). WR 65 is the bright object at the bottom, close to the detector edge. The coordinates are galactic.

## 2 WR 65 AND ITS X-RAY LIGHT-CURVE

The coordinates of WR 65 from different sources are compiled in Table 1. The coordinates from Simbad and the USNO-B1.0 catalog agree well with the source location in the *Chandra* HRI-I image. Except for WR 65 there are no other known objects at this position. WR 65 is a probable member of the cluster Pismis 20, which contains one more WR star, WR 67, and has a distance of  $d = 3272 \pm 303 \text{ pc}$  (Turner 1996).

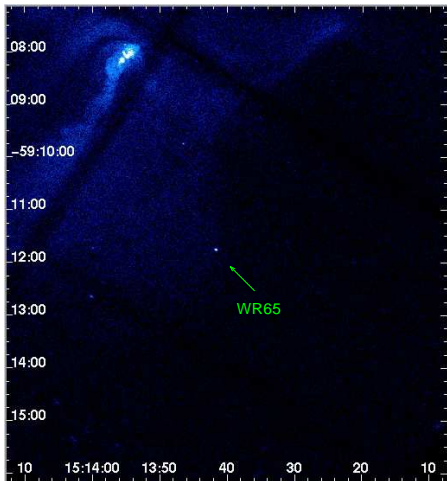
We fit the optical spectrum of WR 65 and its available photometry using the Potsdam Wolf-Rayet (PoWR) stellar atmosphere models (Hamann & Gräfener 2003). The deduced stellar parameters are listed in Table 2.

<sup>\*</sup> E-mail: lida@astro.physik.uni-potsdam.de

**Table 2.** Stellar parameters of WR 65 (from Hamann et al., in prep.)

$E_{B-V}$	$\log L_{\text{bol}}/L_{\odot}^{\text{a}}$	$v_{\infty}$ [km s $^{-1}$ ]	$\dot{M}$ [ $M_{\odot}$ yr $^{-1}$ ] <sup>b</sup>
2.4	5.8...6.4	$\approx 2000$	$10^{-4.6}$ ... $10^{-4.1}$

(a) depending on the adopted reddening law

(b) assuming a clumping contrast  $D = 10$ **Figure 2.** Archival *Chandra* ACIS-I image (0.2-12.0 keV) of WR 65. The observation is from 18 Oct. 2005. The bright object in the upper-left corner of the image is the pulsar PSR B1509-58. WR 65 is projected onto the outskirts of the pulsar wind emission. The coordinates are equatorial (J2000). North up, east left.

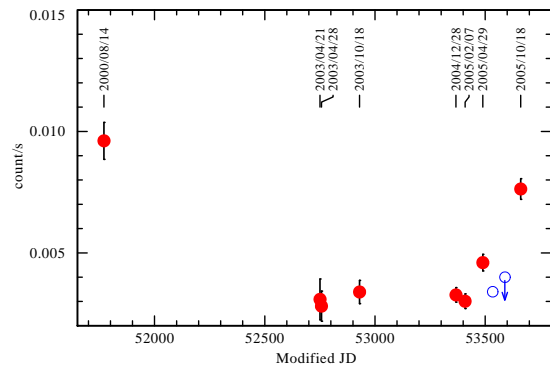
A wind-blown bubble with a radius of  $7'$  is known around WR 65 (Marston 1997). Giacani & Dubner (2004) discovered a H I shell with a radius of 22 pc surrounding WR 65 and WR 67. The infrared *Spitzer* IRAC image of WR 65 at  $8\mu\text{m}$  is shown in Fig. 1. Despite its unfavorable location close to the edge of the detector, a rather compact nebula around WR 65 is visible. The radius of the nebula is  $\approx 1.5'$  or 1.4 pc. Given the strong mass-loss rate of WR 65 and its strong UV field, it is plausible that the nebula is physically associated with this star.

In the X-ray sky, WR 65 is located in a very interesting neighbourhood (see Fig 2). The star is  $7.4'$  away from the supernova remnant (SNR) G320.4-1.2 and  $4'$  away from the X-ray bright ‘‘Cir Pulsar’’ and its associated pulsar wind nebula (PWN). The SNR and the Cir pulsar are at the distance  $d = 5.2 \pm 1.4$  kpc (Gaensler et al. 2002). This region of the sky is often observed, and serendipitous X-ray observations of WR 65 are in archives.

The most homogeneous data set found in archives is from *Chandra* ACIS-I observations conducted from year 2000 to 2005. In 2005 WR 65 was also observed on one occasion by *Chandra* HRC-I and twice by *XMM-Newton*, but was not detected during *XMM-Newton* observations affected by high radiative background.

The local X-ray background is high because WR 65 is projected on the peripheral region of the PWN mentioned above. Therefore we paid special attention to the background subtraction. Conveniently, the X-ray emission from the PWN is well studied (Gaensler et al. 2002; Yatsu et al. 2005). DeLaney et al. (2006) find that it is constant over at least twelve years. We defined background regions as annuli around a stellar point source.

Figure 3 shows the background-subtracted X-ray light-curve of WR 65 that displays a surprisingly high level of variability. Such strong X-ray variability in massive stars is observed only in binary

**Figure 3.** X-ray (0.4-10.0 keV) light-curve of WR 65. The red dots show *Chandra* ACIS-I count-rates. The blue dots show count-rates converted to ACIS-I rates from *Chandra* HRC-I and *XMM-Newton* MOS (upper limit).

systems (Corcoran et al. 2005; Oskinova, Clarke & Pollock 2001). The WR 65 X-ray light curve gives strong evidence that the star is a colliding wind binary (CWB). Unfortunately, the light-curve is too sparse to search for the period. Given the time interval between the two recorded maxima, one may conclude that the period is not longer than about five years.

### 3 WR 65: X-RAY SPECTRAL VARIABILITY

Five of the *Chandra* observations of WR 65 yielded enough counts for a crude X-ray spectral analysis. The background-subtracted spectra obtained at different epochs are displayed in Fig. 4. The spectral energy distribution is harder than for single WR stars (Ignace, Oskinova & Brown 2003). The unresolved emission features coincide with the location of lines of Fe, Ca, Ar, S, Si, and Mg (cf. Figs. 4, 5) in collisionally ionized X-ray spectra. Interestingly, the iron lines at  $\approx 6.7$  keV ( $1.8\text{ \AA}$ ) are weaker at some epochs compared to others (e.g. they seem to disappear completely on 2005 February 07). If real, this may reflect the change of the temperature in the hot plasma.

The X-ray spectrum of WR 65 in high states displays strong emission features in the 2-4  $\text{\AA}$  range (see top panel in Fig. 4). Weak lines of Ca XIX ( $\lambda 3.2\text{ \AA}$ ), Ca XX ( $\lambda 3.0\text{ \AA}$ ), and Ar XVIII ( $\lambda 3.7\text{ \AA}$ ) are sometimes observed in the X-ray spectra of CWBs, e.g. the WC8 binary  $\gamma^2$  Vel (Schild et al. 2004), the WN6 binary WR 25 (Raassen, van der Hucht & Mewe 2003), and the LBV binary  $\eta$  Car (Hamaguchi et al. 2007). It seems plausible to assume that the unresolved Ca and Ar lines contribute to the emission ‘‘bump’’ at 2-4  $\text{\AA}$  in the WR 65 spectrum. However, the strength of this emission complex in WR 65 is much higher than observed in any other CWB. We rule out its origin from the background PWN emission, because there are no emission features at 2-4  $\text{\AA}$  in the spectra extracted from an annulus region around WR 65.

In colliding wind binaries consisting of an OB star and a WC star, the latter has a significantly denser, C, O-enriched wind that is basically opaque for X-rays (Oskinova et al. 2003). When in the course of the orbital motion the wind collision region (WCR) is at superior conjunction relative to the WC star (with respect to the observer), the X-rays generated in the WCR suffer strong absorption. Despite many still unclear details, this general picture is observationally confirmed by the X-ray spectral analysis of the WC+O type binaries WR 140 and  $\gamma^2$  Vel. In these systems the strongest photo-attenuation is seen in low X-ray states, while the lowest photo-

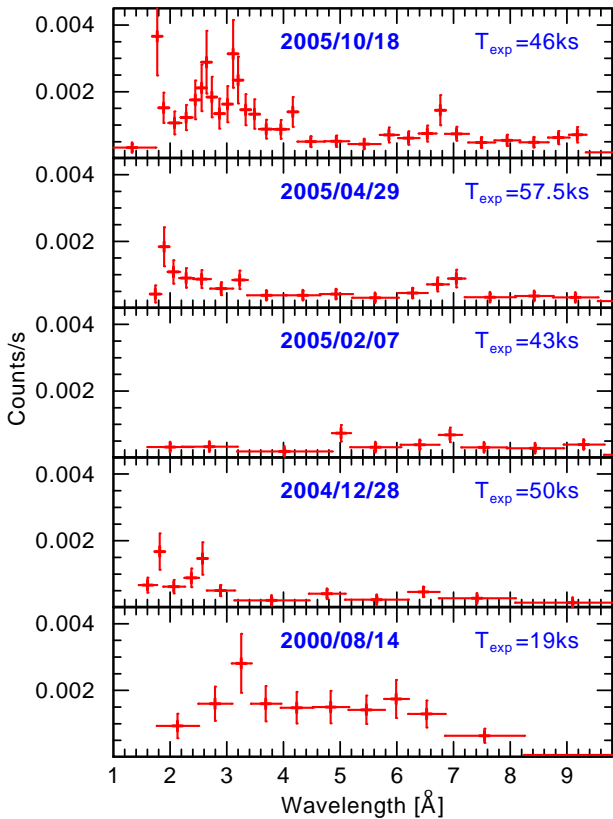


**Figure 4.** *Chandra* ACIS-I background subtracted spectra of WR 65 at different epochs. The date of the observation and the exposure time are given in each panel.

attenuation is found when the X-ray flux is high (Rauw et al. 2000; Schild et al. 2004; Pollock et al. 2005).

To investigate how X-ray spectral variations are coupled with the variation of the absorption column, we fit a model to the observed spectra and check how the model parameters vary between the different epochs.

Following a method used in Pollock et al. (2005) to successfully analyze X-ray spectra of WR 140, we tried to fit the observed WR 65 spectra alternatively with non-equilibrium ionization,  $\rho$ SHOCK, and power-law models using the *xSPEC* software (Arnaud 1996). However, no meaningful constraints on model parameters could be obtained because of the poor quality of the WR 65 spectra. Zhekov (2007) found that only models with non-equilibrium ionization can reproduce the *detailed* X-ray spectra of CWBs. However, he noticed that these spectra can be crudely described by thermal plasma emission with some “average” temperature. Finally, we select a two-temperature thermal plasma model (Smith et al. 2001, *APEC*) where each component is allowed to suffer different degrees of attenuation – the “2T2 $N_H$ ” model. This model provides a first insight into the properties of the system by constraining the model parameters. We refer to the plasma with lower temperature  $kT_1$  as the “soft” model component, and to the plasma with higher temperature  $kT_2$  as the “hard” model component. As demonstrated in Figs. 6, 7 the 2T2 $N_H$ -model sufficiently well reproduces the shape of the WR 65 spectra observed at different epochs.

We assume solar composition. Selecting WC-wind abundances results in scaling down of the parameter that describes normalization of the emission measure (EM), but the effect of abun-

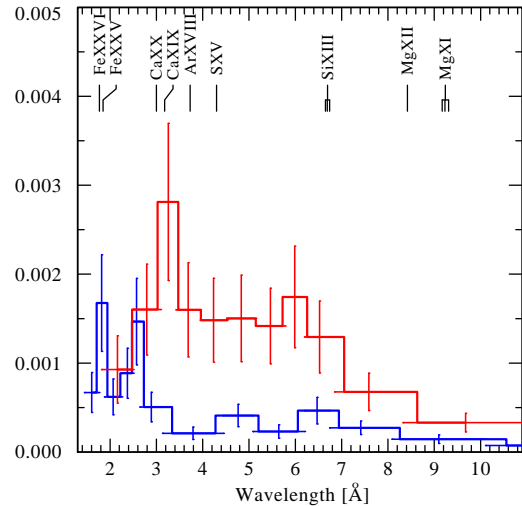


**Figure 5.** *Chandra* ACIS-I spectra of WR 65 in high (red) and low (blue) states (obtained on 2000/08/14/ and 2004/12/28 respectively). Wavelengths of strong spectral lines are indicated.

dances on *spectral shape* cannot be discriminated given the poor quality of available data.

The spectrum of WR 65 with highest signal-to-noise and its best-fit model are shown in Fig. 6. The temperatures inferred from spectral fitting are  $kT_1 = 1.0 \pm 0.2$  keV and  $kT_2 = 13.4 \pm 7.3$  keV. Such temperatures can be expected from the collision of metal enriched winds in wide binaries. The temperature is highest at the point of head-on collision, and is decreasing along the shock cone (Stevens, Blondin & Pollock 1992).

The interstellar absorption column density towards the Cir pulsar,  $N_{H,ism} = 1 \times 10^{22}$  cm $^{-2}$ , is well constrained and is consistent with the color excess inferred from our fitting of the WR 65 spectral energy distribution. The neutral hydrogen column densities are  $N_{H,1} = (2.3 \pm 0.3) \times 10^{22}$  cm $^{-2}$  for the soft component and  $N_{H,2} = (12.2 \pm 4.1) \times 10^{22}$  cm $^{-2}$  for the hard component. The column density to the soft component,  $N_{H,1}$ , exceeds the interstellar column by a factor of more than two, but it is lower than the column density to the hard component,  $N_{H,2}$ . This indicates that the hotter plasma is more deeply embedded.

From the spectrum obtained at 2005/10/18 the model flux is  $F_X(0.6 - 9.0$  keV) =  $1.2 \times 10^{-13}$  erg s $^{-1}$  cm $^{-2}$ , which corresponds to  $L_X = 1.1 \times 10^{32}$  erg s $^{-1}$ , or in terms of stellar bolometric luminosity to  $\log L_X/L_{bol} = -7.2 \dots -7.8$ . The flux of the soft spectral component,  $F_X(0.6 - 2.0$  keV) =  $8.3 \times 10^{-15}$  erg s $^{-1}$  cm $^{-2}$ , corresponds to  $L_X(0.6 - 2.0$  keV) =  $1.0 \times 10^{31}$  erg s $^{-1}$  which is similar to the X-ray luminosity of a single O dwarf (Oskinsonova 2005).

Spectra observed at other epochs were also fitted with the 2T2 $N_H$ -model. For illustration, the spectrum obtained in the low state and its corresponding best-fit model are shown in Fig. 7. Figure 8 shows the model parameters depending on the time of observation. Within the error bars, the temperatures  $kT_1$  and  $kT_2$ , and the absorption column to the source for the soft component,  $N_{H,1}$  are similar at all observed epochs, and therefore are not plotted in Fig. 8. In contrast, the column density to the hard component,  $N_{H,2}$ , changes at different epochs (panel A of Fig. 8). Variations in the EM of the hard and soft components are shown in panels B and C of Fig. 8. The EM of the soft component changes strongly, reflecting the X-ray light-curve variations, while the changes in the EM of the hard component are less pronounced.

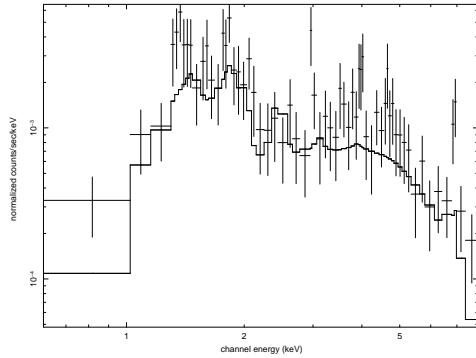


**Figure 6.** ACIS-I spectrum of WR 65 obtained on 2005/10/18 and the best fit spectral model –  $tbabs(N_{H,1}) * apec(kT_1) + tbabs(N_{H,2}) * apec(kT_2)$ . The XSPEC spectral fitting package was used. For the model parameters see text.

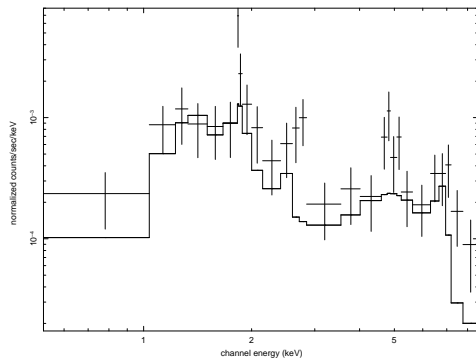


**Figure 7.** Same as in Fig. 6 for the spectrum obtained on 2004/12/28.

#### 4 DISCUSSION

The main findings from the analysis of WR 65 X-ray spectra obtained at different epochs are: (i) the spectra display emission features at the wavelengths of the lines of strongly ionized Fe, Ca, Ar, S, Si, and Mg; (ii) the star shows strong spectral X-ray variability; (iii) the spectra can be fitted with a two-temperature model, consisting of a soft component with  $0.3 \leq kT_1 \leq 1.5$  keV and a hard component with  $2 \leq kT_2 \leq 20$  keV; (iv) the absorption for the hard component is strong and variable, while the absorption for the soft component is less severe and nearly constant; (v) the changes in the EM are stronger for the soft component.

Can these observations be explained in the framework of a colliding wind model? Corcoran et al. (2005) compare the 2.0–10.0 keV light curves of WR 140 and  $\eta$  Car (both are systems with high eccentricity and high inclination) and note that they are very similar. Pittard et al. (1998) explain the light-curve (2.0–10.0 keV) of  $\eta$  Car using a hydrodynamic simulation of colliding winds. They show that the data are broadly consistent with the X-ray emission being moderately low throughout most of the orbit. However, a sharp peak occurs near periastron, when a greater fraction of the stellar winds collides, and the higher pre-shock densities and the lower pre-shock velocities result in stronger radiative cooling. The eclipse occurs immediately after periastron passage when the companion of  $\eta$  Car swings behind the LBV star with its dense wind.

It is hard to see how a similar model can be used to explain the X-ray variability of WR 65. Strong variations in the absorbing column indicate that the orbit of WR 65 has high inclination too. Considering the light-curve (Fig. 3) we can rule out that WR 65 has a period of a few days: the two data points obtained in April 2003

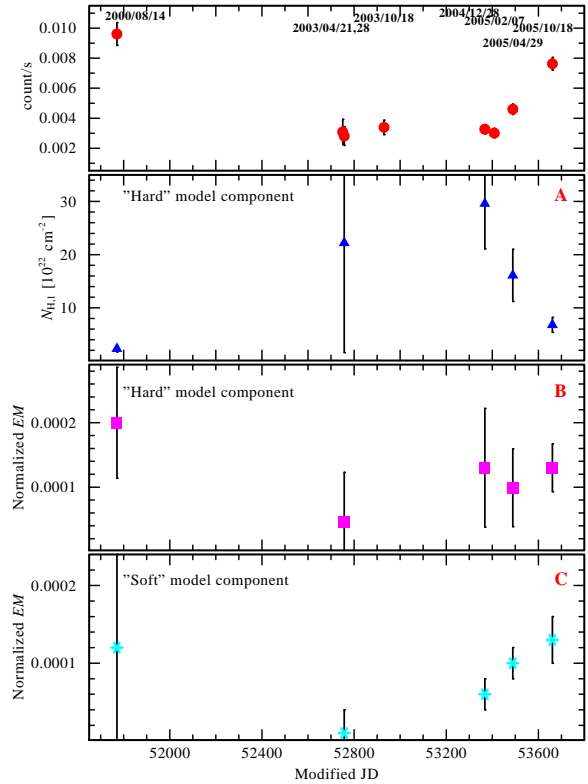


**Figure 8.** Upper panel same as in Fig. 3. Panel A: variations of absorption column density of the hard component obtained from spectral fits. Panel B: normalization factor that characterizes the emission measure of the hard component. Panel C: normalization factor of the soft component.

indicate constant count rates over at least a week. Moreover, two data points in the light-curve separated by two months (12/2004 and 02/2005) are similar, while there is an increase of emission by nearly 70% in the next two months. Therefore, WR 65 has most likely an orbital period of a few years. In this case the long duration of the minimum is inconsistent with its interpretation as attenuation by the wind of the WC star immediately after periastron passage. Quite different from the short-duration rise of column density observed in WR 140 and  $\eta$  Car, the column density in WR 65 is persistently very high,  $N_{H,2} \geq 10^{23}$  cm $^{-2}$ , sharply decreasing only at the maximum X-ray light.

The temporary variations of column density in WR 65 are similar to those measured in the WC8+O binary  $\gamma^2$  Vel (Rauw et al. 2000). Its hard X-ray emission increases by a factor of  $\sim 4$  when column density decreases by factor of  $\sim$  few during the passage of weak-wind inner side of the shock cone across the line of sight (Willis, Schild & Stevens 1995; Rauw et al. 2000; Schild et al. 2004).

In WR 65 the soft X-ray emission is present at all observed epochs. Its variation can be explained by changing emission measure, while the absorption is nearly constant and comparably low. A soft spectral component in the low state is also observed in  $\gamma^2$  Vel, V444 Cyg and  $\eta$  Car. The origin of soft X-rays in these stars is attributed either to individual stellar winds or to a circumstellar nebula. Accordingly, in these objects the absorbing column to the soft component is similar to the interstellar absorbing column. In contrast, we find for WR 65 that  $N_{H,ism} < N_{H,1} < N_{H,2}$ , and the EM of the soft component changes with the X-ray light-curve. Thus it is

unlikely that the intrinsic wind emission of a companion is solely responsible for the soft X-rays from WR 65.

WR 65 is a persistent dust maker (van der Hucht 2001). Monnier et al. (2002) notice that binary stars that are persistent dust makers have nearly circular orbits. We can assume that the same holds for WR 65. There is a growing number of WC9d binary stars that constitute the “pinwheel” class of objects (Tuthill et al. 2008; Marchenko & Moffat 2007). In these binary systems the dust is formed in the wind collision region and is distributed along a wide (compared to the orbital separation) Archimedean spiral. The peak of dust production occurs at some distance downstream from the colliding wind stagnation point.

So far there is no direct evidence that WR 65 is a pinwheel. However, the topology and structure of circumstellar matter in a pinwheel could help to explain X-ray spectral variability in WR 65. Wilms, Allen & McCray (2000) presented a model for the absorption of X-rays that includes a treatment of dust grains. Their work confirmed that large-grain absorption for soft X-rays ( $< 2$  keV) is reduced due to the self-blanketing of grains. Interestingly, from the point of view of radiative transfer this is identical to the reduction of opacity for the X-rays in clumped stellar winds (Feldmeier, Oskinova & Hamann 2003). Winds of WC stars are extremely rich in C and O and could have enhanced abundance of Mg and Ne. C and O are dominant absorbers for the softer X-rays ( $< 1$  keV), while Mg and Ne strongly contribute to the absorption of harder X-rays ( $> 1$  keV). In the dusty shell around a WC9d star, C would be depleted from the gaseous phase and form grains, reducing the opacity for the softer X-rays. This may help to explain the large differences between the column densities that we determine from soft and hard X-rays.

Recently, Lemaster, Stone & Gardiner (2007) presented 3-D hydrodynamical simulations of colliding winds. Scaling the results of their simulation to the parameters of WR 65, soft X-ray emission could originate from a large volume extending above the orbital plane. This emission would show little variation with orbital phase and suffer comparably mild absorption in the outer regions of the WC star wind, similarly to what is observed in WR 65. On the other hand, a high postshock temperature of  $kT \approx 10$  keV is predicted for a confined region near the point where the winds collide head-on. Densities up to  $\rho \geq 10^{-14}$  g cm $^{-3}$  can be expected in the dusty spiral arms. Assuming the wind opacity for hard X-rays as  $\kappa \approx 5$  cm $^2$  g $^{-1}$  (Antokhin, Owocki & Brown 2004), a spiral arm width of  $10^{14}$  cm would explain the observed high absorption. This width is consistent with the observed width of the dusty spiral arms in WR 104 (Tuthill et al. 2008). The lowest absorbing column can be expected at the phase when the line of sight crosses only the outer low density part of the spiral arms. It is possible that the *Chandra* observations of WR 65 at high state have caught this orbital phase.

To conclude, our first brief study of the variable X-ray emission from WR 65 indicates that it is a colliding wind system, where the dust and complex geometry of its colliding wind region are pivotal in explaining its X-ray properties. At present, WR 65 is the only known WC9d star where X-ray emission is detected. Future observations are needed to constrain the orbital parameters of WR 65 and allow for detailed modeling.

## ACKNOWLEDGMENTS

The authors are grateful to P. M. Williams for initiating this study and to N. S. Schulz for useful discussions on the ACIS-I spectra. The authors thank the referee (A. F. J. Moffat) for detailed and help-

ful comments. Based on *Chandra* data: obsid 754, 6117, 6116, 5535, 5534, 5515, 4384, 3834, 3833. This research has made use of software provided by the Chandra X-ray Center and data obtained through the NASA/IPAC Infrared Science Archive and High Energy Astrophysics Science Archive Research Center. The SIMBAD database, operated at CDS, Strasbourg, France, and NASA’s Astrophysics Data System were extensively used during this work.

## REFERENCES

- Antokhin I. I., Owocki S. P., & Brown J. C., 2004, ApJ, 611, 434  
 Arnaud K.A., 1996, ASPC, 101, 17  
 Chapman J.M., Leitherer C., Koribalski, B., et al., 1999, ApJ, 518, 890  
 Corcoran M. F., Pittard J. M., Stevens I. R., Henley D. B., Pollock A. M. T., 2005, in: X-Ray and Radio Connections, eds. L.O. Sjouwerman and K.K Dyer. Published electronically by NRAO, <http://www.aoc.nrao.edu/events/xraydio>  
 DeLaney T., Gaensler B. M., Arons J., Pivovarov M. J., 2006, ApJ, 640, 929  
 Ignace R., Oskinova L. M., Brown J. C., 2003, A&A, 408, 353  
 Eichler D., Usov V., 1993, ApJ, 402, 271  
 Feldmeier A., Oskinova L., Hamann W.-R., 2003, A&A, 403, 217  
 Gaensler B. M., Arons J., Kaspi V. M., Pivovarov M. J., Kawai N., Tamura K., 2002, ApJ, 569, 878  
 Giacani E., Dubner G., 2004, A&A, 413, 225  
 Hamaguchi K. et al., 2007, ApJ, 663, 522  
 Hamann W.-R., Gräfener G., 2003, A&A, 410, 993.  
 Leitherer C., Chapman J.M., Koribalski B., 1997, ApJ, 481, 898  
 Lemaster M. N., Stone J. M., Gardiner T. A., 2007, ApJ, 662, 582  
 Maeda Y., Koyama K., Yokogawa J., Skinner S., 1999, ApJ, 510, 967  
 Marchenko S. V., Moffat A. F. J., 2007, ASPC, 367, 213  
 Marston A. P., 1997, ApJ, 475, 188  
 Monnier J.D., Greenhill L.J., Tuthill P.G., Danchi W.C. 2002, ApJ, 566, 399  
 Oskinova L. M., Clarke, D., Pollock, A. M. T., 2001, A&A, 378, L21  
 Oskinova L. M., Ignace R., Hamann W.-R., Pollock A. M. T., Brown, J. C. 2003, A&A, 402, 755  
 Oskinova L. M., 2005, MNRAS, 361, 679  
 Pittard J. M., Stevens I. R., Corcoran M. F., Ishibashi, K., 1998, MNRAS, 299, L5  
 Pittard J. M., 2007, ApJ, 660, L141  
 Pollock A. M. T., Corcoran M. F., Stevens I. R., Williams P. M., 2005, ApJ, 629, 482  
 Raassen A. J. J., van der Hucht K. A., Mewe R., et al., 2003, A&A, 402, 653  
 Rauw G., Stevens I. R., Pittard J. M., Corcoran M. F., 2000, MNRAS, 316, 129  
 Schild, H., Güdel, M., Mewe, R., et al. 2004, A&A, 422, 177  
 Smith R. K., Brickhouse N. S., Liedahl D. A., Raymond J. C., 2001, ApJ, 556, L91  
 Stevens I. R., Blondin J. M., Pollock A. M. T., 1992, ApJ, 386, 265  
 Turner D. G., 1996, AJ, 111, 828  
 Tuthill P. G., Monnier J. D., Lawrance N., Danchi W. C., Owocki S. P., Gayley K. G., 2008, ApJ, 675, 698  
 Wallace D. J., 2007, ASPC, 367, 37  
 van der Hucht K. A., 2001, New Astron. Rev., 45, 135

- Williams P. M., van der Hucht K. A., Thé P. S., 1987, *A&A*, 182, 91
- Williams P. M., van der Hucht K. A., Pollock A. M. T., et al., 1990, *MNRAS*, 243, 662
- Willis A. J., Schild H., Stevens, I. R., 1995, *A&A*, 298, 549
- Wilms J., Allen A., McCray R., 2000, *ApJ*, 542, 924
- Yatsu Y., Kawai N., Kataoka J., Kotani T., Tamura K., Brinkmann W., 2005, *ApJ*, 631, 312
- Zhekov S. A., 2007, *MNRAS*, 382, 886
- Zubko V. G., 1998, *MNRAS*, 295, 109